

# Analytical Methods

Accepted Manuscript



This is an *Accepted Manuscript*, which has been through the RSC Publishing peer review process and has been accepted for publication.

*Accepted Manuscripts* are published online shortly after acceptance, which is prior to technical editing, formatting and proof reading. This free service from RSC Publishing allows authors to make their results available to the community, in citable form, before publication of the edited article. This *Accepted Manuscript* will be replaced by the edited and formatted *Advance Article* as soon as this is available.

To cite this manuscript please use its permanent Digital Object Identifier (DOI®), which is identical for all formats of publication.

More information about *Accepted Manuscripts* can be found in the [Information for Authors](#).

Please note that technical editing may introduce minor changes to the text and/or graphics contained in the manuscript submitted by the author(s) which may alter content, and that the standard [Terms & Conditions](#) and the [ethical guidelines](#) that apply to the journal are still applicable. In no event shall the RSC be held responsible for any errors or omissions in these *Accepted Manuscript* manuscripts or any consequences arising from the use of any information contained in them.

**Sensitive electrochemical determination of promethazine hydrochloride based on the poly(*p*-aminobenzene sulfonic acid)/flowerlike ZnO crystals composite film**

**Yanling Chen , Honghui Liu , Yunchun Liu , Zhousheng Yang \***

College of Chemistry and Materials Science, Anhui Key Laboratory of Chemo-Biosensing, Anhui Normal University, Wuhu 241000, People's Republic of China

---

\*Corresponding author: Fax: +86-553-3869303. E-mail address: [yzhoushe@mail.ahnu.edu.cn](mailto:yzhoushe@mail.ahnu.edu.cn) (Z. S.

Yang).

**Abstract:** ZnO crystals were synthesized by a hydrothermal decomposition process in the presence of poly(vinylpyrrolidone) as the surfactant, then characterized by scanning electron microscopy and X-ray diffraction. The composites of flowerlike ZnO combined with poly(*p*-aminobenzene sulfonic acid) (*p*-ABSA) were immobilized on a glassy carbon electrode for constructing a sensitive electrochemical sensor. The electrocatalytic response to PHZ on the prepared sensor was measured using cyclic voltammetry and differential pulse voltammetry (DPV) in PBS buffer (pH 8.0). The fabricated sensor was successfully used for the detection of promethazine hydrochloride (PHZ) in a 0.10 M phosphate buffer solution (PBS) at pH 8.0. Under optimal conditions, the linear concentration range of PHZ obtained at *p*-ABSA/ZnO composite film using DPV technique was 0.01  $\mu\text{M}$  to 59.84  $\mu\text{M}$  ( $R = 0.997$ ) and the detection limit was 0.004  $\mu\text{M}$  at  $S/N = 3$ . Furthermore, the prepared sensor displayed voltammetric responses with excellent reproducibility, high sensitivity and stability for PHZ. Therefore, the *p*-ABSA/ZnO composite film has become a promising application for quantitative determination of PHZ.

**Keywords:** Flowerlike ZnO · Poly(*p*-aminobenzene sulfonic acid) · Promethazine Hydrochloride · Electrochemical sensor

## 1 Introduction

Recently, the use of different nano-sized metal and semiconductor materials for the design of sensors and biosensors has received considerable attention due to the fact they have chemical, physical and electronic properties that are different from those of bulk materials.<sup>1,2</sup> Among these nanostructured materials, more and more attention was paid to metal oxide semiconductors in bioanalytical area as they possess properties like high surface area, non-toxicity, ease of fabrication, optical transparency, chemical stability.<sup>3</sup>

ZnO crystals as a versatile semiconductor nano-material have great prospective application in biosensors due to their biomimetic feature.<sup>4</sup> The research results revealed that the morphology and structure of nano-materials have important effects on their properties, which determines their applications in many fields. Lots of ZnO nanostructures have attracted considerable interest in biosensor applications due to their distinguished performance, such as needles grown on the annealed nanotubes using hydrothermal method,<sup>5</sup> forks used for rapid and ultrahigh sensitive determination of hydrogen peroxide ( $\text{H}_2\text{O}_2$ ),<sup>6</sup> porous nanosheets for the detection of  $\text{H}_2\text{O}_2$  and  $\text{NaNO}_2$  sensitively,<sup>7</sup> flowers synthesized through a wet chemical route, then combined with horseradish peroxidase which displayed an enhanced electrocatalytic activity towards the reduction of  $\text{H}_2\text{O}_2$  and nanorods for detection of phenolic compounds.<sup>8,9</sup>

However, metal nanoparticle suspensions are unstable in solution which inhibits their applications due to their irreversible aggregation over time. Certain catalytically

active metal particles supported by some conducting polymers have overcome this difficulty and fulfilled several functions, which may be due to that conducting polymers have good stability, reproducibility, more active sites and homogeneity. Conducting polymer and nanoparticles (NPs) composites have already been reported in the literature, such as PTH/AuNPs/HRP for detection of  $H_2O_2$ ,<sup>10</sup> PPy/Au which has greater conductivity and better stability than PPy,<sup>11</sup> GR-TiO<sub>2</sub>/PABSA used for simultaneous electrochemical determination of dopamine and tryptophan,<sup>12</sup> SiW<sub>12</sub>/CNTs/PAn for the sensitive amperometric determination of ascorbic acid<sup>13</sup> and PAMAM/Fe<sub>3</sub>O<sub>4</sub> for determination of bisphenol A.<sup>14</sup>

Promethazine hydrochloride (N,N-dimethyl-1-phenothiazin-10-yl-propan-2-amine hydrochloride) (PHZ) is a prominent compound in the large group of phenothiazine derivatives widely used for its antihistaminic, sedative, antipsychotic, analgesic and anticholinergic properties.<sup>15,16</sup> However, adverse effects caused by PHZ in humans have also attracted enormous attention, such as cardiac, reproductive alterations, endocrinal, occasional hypotension and so on.<sup>17</sup> Therefore, its determination in commercial formulations is extremely important. Up to now, many analytical techniques have been reported for the determination of PHZ, such as chemiluminescence,<sup>18</sup> high performance liquid chromatography,<sup>19,20</sup> capillary zone electrophoresis.<sup>21</sup> However, most of these methods are complicated, time consuming and also require expensive instrumentation. Recently, electroanalytical techniques have been employed to determine PHZ, since they are simple, cost little, and require relatively short analysis times.<sup>22,23</sup>

In this work, ZnO crystals with flowerlike structure have been synthesized using PVP as surfactant through the hydrothermal method. A novel composite material which combined *p*-ABSA with flowerlike ZnO was constructed on the surface of GCE to form a biosensor for the determination of PHZ. Based on the excellent synergistic effect between ZnO and *p*-ABSA, the biosensor exhibited attractive performances in that it enhanced significantly the oxidation peak current of PHZ and lowered the oxidation potential.

## 2 Experimental

### 2.1 Reagents and apparatus

Promethazine hydrochloride was purchased from Sigma. A promethazine stock solution was prepared by dissolving suitable amounts of promethazine hydrochloride in ultrapure water and stored in a refrigerator at 4°C. Standard solutions were then prepared from this stock solution by serial dilution as required. Para-aminobenzene sulfonic acid was purchased from Wulian Chemical Industry Factory (Shanghai, China). The buffer solutions were prepared from 0.10 M Na<sub>2</sub>HPO<sub>4</sub> and NaH<sub>2</sub>PO<sub>4</sub> aqueous solution. Other chemicals were of analytical grade and used without further purification. Ultrapure water was used throughout the experiments. All the experiments were carried out at room temperature.

All electrochemical measurements were performed with a CHI 660A electrochemical work station (Chenhua Instruments Co., Shanghai, China). A conventional three-electrode cell was used, including glassy carbon electrode (diameter 3 mm) as the working electrode, Ag/AgCl electrode with saturated KCl as a

reference electrode and platinum (Pt) wire as the counter electrode. The scanning electron microscope (SEM) image was obtained on S-4800 field emission scanning electron microanalyser (Hitachi, Japan). Powder X-ray diffraction (XRD) of ZnO was carried out on a Shimadzu XRD-6000 X-ray diffractometer operating with Cu-K $\alpha$  radiation ( $\lambda=0.154060$  nm), employing a scanning rate of  $0.02^\circ\text{s}^{-1}$  and  $2\theta$  ranges from  $20^\circ$  to  $70^\circ$ .

## 2.2 Preparation of ZnO crystals

In a typical synthesis, 0.21 g Zn(Ac) $_2\cdot 2\text{H}_2\text{O}$  was mixed with 5.0 M NaOH under ultrasonication condition, resulting in a transparent  $[\text{Zn}(\text{OH})_4]^{2-}$  solution. Then, 0.2 g PVP was added into above solution followed by constant stirring. The mixture was put into a Teflon lined steel autoclave and heated at  $180^\circ\text{C}$  for 13 h. When the product was cooled down to room temperature, it was isolated by centrifuge, washed several times with ethanol and distilled water, and then dried at  $100^\circ\text{C}$ .

## 2.3 Preparation of modified electrodes

A glassy carbon electrode was mirror polished on chamois leather with Al $_2\text{O}_3$  slurry, and cleaned thoroughly in an ultrasonic cleaner with nitric acid solution, alcohol and water, respectively. The GCE was coated with 5  $\mu\text{L}$  of the resulting 2.8 mg/mL ZnO suspension and allowed to dry under infrared lamp for 2 min. Then, the ZnO modified GCE was treated in *p*-ABSA solution (2 mM) and 0.10 M phosphate buffer solution (pH 7.0) by cyclic voltammetry between  $-1.2$  and  $2.4$  V at  $100$  mV  $\text{s}^{-1}$

for eight cycles according to the reference.<sup>12</sup> Afterwards, the film was washed with water to remove physically adsorbed material and the *p*-ABSA/ZnO/GCE was obtained.

## 2.4 Analytical procedure

Cyclic voltammetry and differential pulse voltammetric measurements were carried out with three electrodes in phosphate buffer solution. The CVs were recorded by cycling the potential between 0.2 V and 1.0 V at a scan rate of 100 mVs<sup>-1</sup>. Because the differential pulse voltammetry has excellent sensitivity and selectivity, it is selected as the analytical technique by applying a sweep potential from 0.15 V to 0.95 V. The parameters are as follows: pulse amplitude, 0.2 V; pulse width, 0.05 s; sample width, 0.0167s; pulse period, 0.2 s; quiet time, 2 s.

## 3 Results and discussion

### 3.1 Characterization of ZnO crystals and the modified electrodes

The structure and morphology of the resulting ZnO and *p*-ABSA/ZnO were characterized using SEM. Fig. 1 displays typical SEM images of the ZnO (Fig.1a,b), *p*-ABSA/ZnO (Fig.1c,d). As can be seen from the low (Fig.1b) and high (Fig.1a) magnification SEM image, the ZnO crystals show flowerlike structures built up by many sheets which are smooth. The sizes of these sheets are not uniform, and their lengths are several microns. Fig. 1c and Fig. 1d show the high and low magnification SEM image of the *p*-ABSA/ZnO, on which a pattern of thin film is observable which

consisted of particles and the flowerlike ZnO become intransparent. It can be seen that the ABSA has been deposited onto the surface of GCE along with ZnO.

**Fig. 1**

XRD analysis was used to determine the structure and phase of the flowerlike ZnO. Figure.2 is the XRD pattern of the product prepared by hydrothermal synthesis method. All diffraction peaks can be perfectly indexed to the wurtzite-type (space group P63mc) ZnO (JCPDS no. 75-576). The strong and sharp diffraction peaks indicate that the product has good crystallinity. No characteristic peaks belonging to impurities are observed, which implies that pure ZnO products were obtained.

**Fig. 2**

To characterize the electron transfer properties of the different modified electrodes, electrochemical impedance spectroscopy (EIS) was used. In electrochemical impedance measurement, the semicircular part at higher frequency corresponds to the electron-transfer process, and the diameter is equivalent to the electron transfer resistance ( $R_{et}$ ), which controls the electron transfer kinetics of the redox probe at the electrode surface. The linear part in the EIS represents the diffusion-limited process. Fig. 3 shows the impedance spectra at 0.18 V represented as Nyquist plots for bare GCE (a), ZnO/GCE (b) and *p*-ABSA/ZnO/GCE (c) using 5 mM  $\text{Fe}(\text{CN})^{-3}/\text{Fe}(\text{CN})^{-4}$  containing 0.1 M KCl as probe. For the bare GCE, the value of electron transfer resistance was 272.9  $\Omega$ . When ZnO was immobilized on the GCE surface (ZnO/GCE), it can be seen that a big well defined semi-circle at higher frequencies was obtained, indicating large interfacial impedance. When *p*-ABSA was deposited on the surface of

ZnO/GCE, the impedance value obtained at *p*-ABSA/ZnO/GCE was smaller than that at GCE, which could be attributed to the conductivity of *p*-ABSA and electrostatic adsorption between positively charged *p*-ABSA and  $\text{Fe}(\text{CN})^{-3}/\text{Fe}(\text{CN})^{-4}$  leading to a lower interfacial electron resistance, and demonstrated that *p*-ABSA/ZnO film was successfully immobilized on the GCE surface.

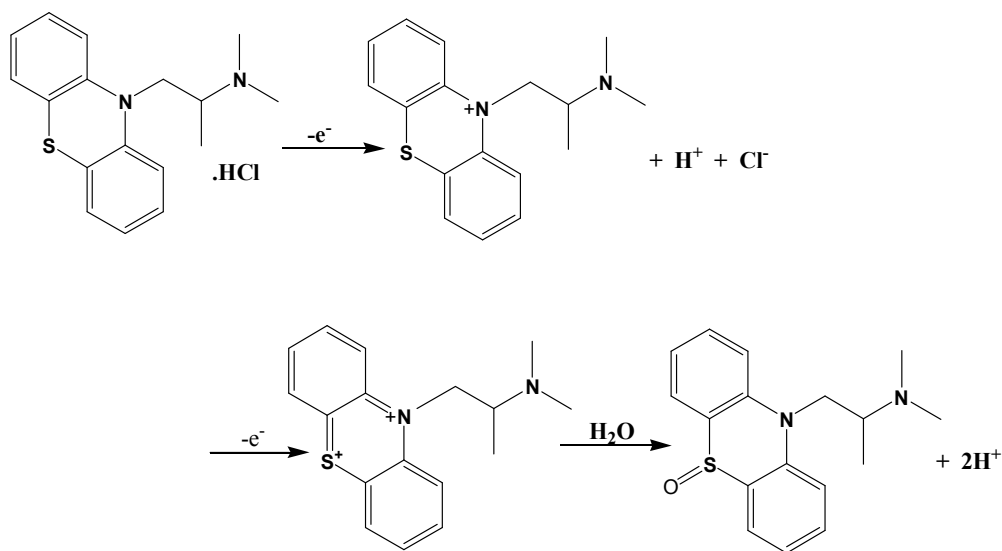
**Fig. 3**

### 3.2 Electrochemical behavior of promethazine on the modified electrode

The electrochemical behavior of PHZ at different electrodes in 0.10 M PBS (pH 8.0) was examined by CVs (Figure 4) in the range from 0.2 V to 1.0 V, at a scan rate of 100  $\text{mV s}^{-1}$ . In the absence of PHZ, no redox peak was observed at *p*-ABSA/ZnO/GCE, demonstrating that the *p*-ABSA/ZnO/GCE was non-electroactive in the scanned potential window. Two small oxidation peaks appeared on CV curves using the bare GCE (curve a) and ZnO/GCE (curve b) and no reduction peak was observed in present of PHZ, respectively. As for *p*-ABSA/GCE (curve c), the oxidation currents of PHZ were more obvious than at the bare GCE and ZnO/GCE, the corresponding oxidation peak potential values were 0.524 and 0.786 V for PHZ. Furthermore, the *p*-ABSA/ZnO/GCE (curve d) resulted in excellent amplification of the PHZ oxidation response compared to that at the bare electrode, ZnO/GCE and *p*-ABSA/GCE, with peak potential value shifting negative to 0.501V and 0.735 V, respectively. All the above indicated that the oxidation of PHZ was irreversible on the *p*-ABSA/ZnO surface and the modified electrode possessed good electro-catalytic

activity. The results may be ascribed to the high conductivity, fast electron transfer rate and excellent synergistic effect of *p*-ABSA and ZnO.

According to previous studies of PHZ and other compounds of the same chemical group (phenothiazines),<sup>24,25,26</sup> probable oxidation mechanisms for promethazine on the prepared sensor was inferred as follow. The oxidation process occurs by the removal of one electron from the nitrogen atom, leading to the formation of a relatively stable cation radical (peak B) whose oxidation results in promethazine sulfoxide (peak A).



**Scheme 1** Oxidation mechanisms for Promethazine on the prepared sensor

**Fig. 4**

### 3.3 Effect of modification amounts on oxidation current of PHZ

The electric conductivity of ZnO is poorer compared with the GCE, although

flowerlike ZnO can considerably enhance the oxidation response of PHZ. Therefore, large amount of ZnO certainly lowers the conductivity of the GCE, resulting in low determination sensitivity. The relationship between the oxidation peak current of PHZ and quantities of ZnO was surveyed. Experimental result is shown in Fig.5. The oxidation peak current of PHZ increased gradually with improving ZnO quantity from 5 to 14  $\mu\text{g}/\text{cm}^2$  and then the oxidation peak current conversely decreased with further increasing ZnO quantity from 14 to 28  $\mu\text{g}/\text{cm}^2$ . According to previous work,<sup>7</sup> the amount of nanoparticle will change the effective surface area of electrode, and excess flowerlike ZnO modified on the GCE will gave poor current response. Hence, the quantity of 14  $\mu\text{g}/\text{cm}^2$  ZnO provided reasonable sensitivity in the voltammetric responses, and was selected as the optimum quantity for modification of the electrode surface in this article.

**Fig. 5**

### **3.4 Effects of scan rate and pH on the electrochemical behavior of PHZ**

The effect of scan rate ( $v$ ) on the electrochemical behavior of PHZ was examined in pH 8.0 PBS containing 20  $\mu\text{M}$  PHZ by CVs in the range of 30 to 180  $\text{mV s}^{-1}$ . As can be seen in Fig.6, the oxidation peak currents of PHZ increased with increasing the scan rate while their oxidation peak potentials gradually shifted to positive values. The peak current is proportional to the square root of the scan rates for PHZ with linear regression equations as  $I_{pa} / \mu\text{A} = -3.16921 + 1.24391v^{1/2}$  ( $R = 0.998$ ) for peak B, indicating that the oxidation processes are typical diffusion-controlled

processes.

**Fig. 6**

The influence of solution pH on the electrocatalytic oxidation of PHZ at the *p*-ABSA/ZnO/GCE was explored by CVs in the pH range of 6.0–9.0. As can be seen in Fig. 7 I, the oxidation peak currents of PHZ increase with the solution pH in the range of 6.0–8.0 and reach a maximum value at pH 8.0, then the electrode response started to decrease with higher pH value. The fluctuation can be attributed to the change of electrostatic interaction between *p*-ABSA/ZnO and promethazine due to their protonation. Moreover, the change of electrochemical reaction rate also can produce some effects because it involves proton transfer.<sup>24</sup> Therefore, pH 8.0 was chosen as the optimum pH for the sensitive determination of PHZ.

In addition, the relationship between the peak potential of PHZ and pH was also examined. Fig. 7 II illustrated that the oxidation peak potential of PHZ shifted negatively with the increment of the solution pH, indicating that protons were directly involved in the electrode reaction processes.

**Fig. 7**

### 3.5 Determination of PHZ

Under the optimal conditions, differential pulse voltammetry experiments were performed using poly(*p*-ABSA)/ZnO/GCE in phosphate buffer solution containing various concentrations of PHZ because differential pulse voltammetry has the advantage of an increase in sensitivity and better characteristics for analytical

applications. As shown in Fig.8, the two oxidation peaks for PHZ could be clearly identified at about 0.45 V and 0.68 V with a linear relation between the peak currents and the concentrations. The results showed that the anodic peak currents of PHZ were linearly related to the concentration over the range of 0.01–59.84  $\mu\text{M}$ . The regression equation was  $I_{pa} / \mu\text{A} = -0.56337 + 0.1445C_{\text{PHZ}} / \mu\text{M}$  ( $R = 0.996$ ) for peak B. The detection limit was 0.004  $\mu\text{M}$  at  $S/N = 3$ . The values are comparable with values reported by other research groups for electrocatalytic oxidation of PHZ at the surface of chemically modified electrodes through other mediators (Table 1).

**Fig. 8**

### 3.6 Interference study

For evaluating selectivity of the poly(*p*-ABSA)/ZnO modified electrode, various possible interfering species were tested to examine whether they interfered with the determination of PHZ using this electrode. Several common metal ions, such as  $\text{Cu}^{2+}$ ,  $\text{Fe}^{2+}$ ,  $\text{Ca}^{2+}$ ,  $\text{K}^+$ ,  $\text{Na}^+$ ,  $\text{Mg}^{2+}$  were added into the PBS (pH 8.0). It was found that their interference with the electrochemical reaction under the experimental conditions was negligible for quantitative analysis which may be due to that metal ions are not active in the positive potential range and will not co-deposit with the PHZ. Other organic compounds like ascorbic acid, farina, cane sugar, glucose, nitrobenzene and benzoic acid did not show any interference either in the determination of PHZ which may be due to they are not oxidized under experimental conditions, even at a ratio of 100:1 interference-to- PHZ.

### 3.7 Stability and reproducibility of the poly(*p*-ABSA)/ZnO film

In order to survey the stability of the poly(*p*-ABSA)/ZnO modified electrode, the electrode was stored at 4 °C. After 5 weeks storage, only a small decrease of peak current sensitivity with a relative standard deviation (RSD) of  $1.27 \pm 0.03\%$  for peak B of PHZ was observed, which implies the excellent stability of the modified electrode.

The reproducibility of the poly(*p*-ABSA)/ZnO modified electrode was also investigated. Four freshly prepared modified electrodes have been used for the detection of PHZ, respectively. The relative standard deviation (RSD) for four successive assays was calculated as 3.5%, displaying an acceptable reproducibility.

## 4 Conclusions

The flowerlike ZnO was prepared by hydrothermal synthesis method using PVP as surfactant. The appropriate concentration of PVP plays an important role in the formation of the 3D flowerlike structure. The poly(*p*-ABSA)/ZnO modified electrode was constructed and used for exploring the electrochemical behaviors of PHZ. Remarkable enhancement effects on the oxidation peak currents were observed with the negative shift of the oxidation peak potentials. The results were attributed to the flower-like structure of ZnO and fast electron transfer kinetics of *p*-ABSA. Moreover, the high electrocatalytic activity is attributed to the excellent synergistic effect of *p*-ABSA and ZnO. The nanocomposite may offer a new approach for developing novel types of highly sensitive and stable electrochemical biosensors.

## Acknowledgment

This work was supported by the Natural Science Foundation of China (grant No. 20775002) and Innovative Fund of Anhui Normal University (2012cxjj01).

## References

1. A. Ferancová, S. Rengaraj, Y. Kim, J. Labuda and M. Sillanpää, *Biosens. Bioelectron.*, 2010, **26**, 314 -20.
2. P. P. Dai and Z. S. Yang, *Microchim. Acta*, 2012, **176**, 109 -115.
3. R. Ban, J. J. Li, J. T. Cao, P. H. Zhang, J. R. Zhang and J. J. Zhu, *Anal. Methods*, DOI: 10.1039/c0xx00000x.
4. M. Gao, G. Z. Xing, J. H. Yang, L. L. Yang, Y. J. Zhang, H. L. Liu, H. G. Fan, Y. R. Sui, B. Feng, Y. F. Sun, Z. Q. Zhang, S. S. Liu, S. Li and H. Song, *Microchim. Acta*, 2012, **179**, 315 -321.
5. G. S. Kim, S. G. Ansari, H. K. Seo, Y. S. Kim and H. S. Shin, *J. Appl. Phys.*, 2007, **102**, 084302 - 084302-6.
6. Z. Yang, X. L. Zong, Z. Z. Ye, B. H. Zhao, Q. L. Wang and P. Wang, *Biomater.*, 2010, **31**, 7534 -7541.
7. X. B. Lu, H. J. Zhang, Y. W. Ni, Q. Zhang and J. P. Chen, *Biosens. Bioelectron.*, 2008, **24**, 93 -98.

8. C. L. Xiang, Y. J. Zou, L. X. Sun and F. Xu, *Sens. Actuators, B*, 2009, **136**, 158-162.
9. J. W. Zhao, D. H. Wu and J. F. Zhi, *Bioelectrochem.*, 2009, **75**, 44-49.
10. Q. X. Wang, H. L. Zhang, Y. W. Wu and A. M. Yu, *Microchim. Acta*, 2012, **176**, 279-285.
11. W. Chen, C. M. Li, P. Chen and C. Q. Sun, *Electrochim. Acta*, 2007, **52**, 2845-2849.
12. C. X. Xu, K. J. Huang, Y. Fan, Z. W. Wu, J. Li and T. Gan, *Mater. Sci. Eng. C*, 2012, **32**, 969-974.
13. X. W. Zhang, G. S. Lai, A. M. Yu and H. L. Zhang, *Microchim. Acta*, 2013, **180**, 437-443.
14. H. S. Yin, L. Cui, Q. P. Chen, W. J. Shi, S. Y. Ai, L. S. Zhu and L. N. Lu, *Food Chem.*, 2011, **125**, 1097-1103.
15. G. Sudeshna and K. Parimal, *Eur. J. Pharmacol.*, 2010, **648**, 6-14.
16. T. Alizadeh and M. Akhoundian, *Electrochim. Acta*, 2010, **55**, 5867-5873.
17. J. P. Marcoa, K. B. Borgesa, C. R. T. Tarley, E. S. Ribeiroc and A. C. Pereira, *Sens. Actuators, B*, 2013, **177**, 251-259.
18. S. M. Sultan, Y. A. M. Hassan and A. M. Abulkibash, *Talanta*, 2003, **59**, 1073-1080.
19. M. W. Kosior, A. Skalska, and A. Matysik, *J. Pharm. Biomed. Anal.*, 2006, **41**, 286-289.
20. M. C. Quintana, M. H. Blanco, J. Lacal and L. Hernández, *Talanta*, 2003, **59**,

417-422.

21. D. C. Le, C. J. Morin, M. Beljean, A. M. Siouffi and P. L. Desbène, *J. Chromatogr. A*, 2005, **1063**, 235-240.
22. A. K. Hassan, B. Saad, S. A. Ghani, R. Adnan, A. A. Rahim, N. Ahmad, M. Mokhtar, S. T. Ameen and S. M. A. Araji, *Sensors*, 2011, **11**, 1028-1042.
23. H. Tang, J. H. Chen, K. Z. Cui, L. H. Nie, Y. F. Kuang and S. Z. Yao, *J. Electroanal. Chem.*, 2006, **587**, 269-275.
24. P. Xiao, W. B. Wu, J. J. Yu and F. Q. Zhao, *Int. J. Electrochem. Sci.*, 2007, **2**, 149-157.
25. Y. N. Ni, L. Wang and S. Kokot, *Anal. Chim. Acta*, 2001, **439**, 159-168.
26. D. Daniel and I. G. R. Gutz, *Anal. Chim. Acta*, 2003, **494**, 215-224.
27. F. W. P. Ribeiro, A. S. Cardoso, R. R. Portela, J. E. S. Lima, S. A. S. Machado, P. L. Neto, D. D. Souza and A. N. Correia, *Electroanal.*, 2008, **20**, 2031-2039.

**Table 1** Comparison of the proposed method with other electrochemical methods for the determination of PHZ

Modified electrode	Method	Supporting electrolyte	Linear range ( $\mu\text{M}$ )	Detection limit ( $\mu\text{M}$ )	Ref.
MWCN/SiAlNb/DNA	SWV	PBS 7.0	20–100	5.9	[17]
graphite–BMIMPF <sub>6</sub> /Au	CV	PBS 6.7	0.05–50	--	[19]
(MWCN)/gold electrode	LSV	PBS 4.0	0.05 to 10	0.01	[24]
Glassy carbon electrode	DPSV	BR 9.0	0.312 to 3.12	0.104	[25]
Boron-doped diamond electrodes	SWV	BR 4.0	0.596 to 4.76	0.0266	[26]
Gold electrode	FIA	--	1.0 to 5000	30	[27]
<i>p</i> -ABSA/ZnO/GCE	DPV	PBS 8.0	0.01 to 59.84	0.004	This work

**Figure captions**

**Fig. 1** SEM image of the low and high magnification ZnO crystals (a, b) and *p*-ABSA/ZnO/GCE (c, d)

**Fig. 2** XRD pattern of ZnO crystals

**Fig.3** Nyquist plot of the bare GCE (a), ZnO/GCE (b), *p*-ABSA/ZnO/GCE (c) in 5 mM Fe(CN)<sup>-3</sup>/Fe(CN)<sup>-4</sup> containing 0.1 M KCl

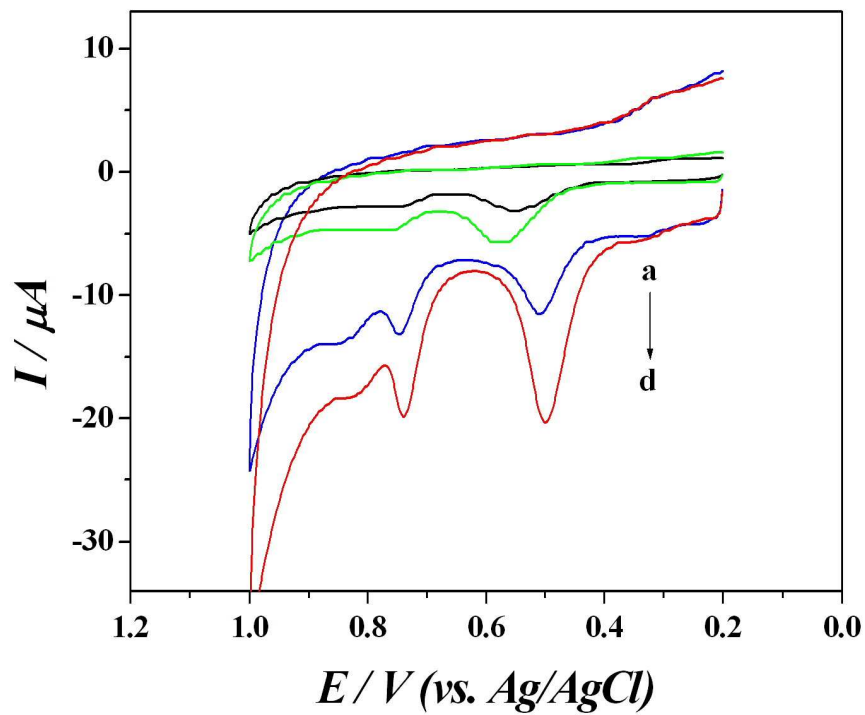
**Fig. 4** Cyclic voltammograms of 80 μM PHZ in 0.10 M PBS (pH 8.0) recorded at the bare GCE (a), ZnO/GCE (b), *p*-ABSA/GCE (c), *p*-ABSA/ZnO/GCE (d). Scan rate is 100 mV s<sup>-1</sup>

**Fig.5** Effect of ZnO concentration on the *p*-ABSA/ZnO/GCE response at constant PHZ concentration in 0.10 M PBS (pH 8.0)

**Fig. 6** CVs of *p*-ABSA/ZnO/GCE in 0.10 M PBS (pH 8.0) containing 20 μM PHZ at the different scan rate of (from a to k): 30, 50, 70, 100, 120, 140, 160, 180 mV s<sup>-1</sup>. The inset shows the linear relationship between the peak currents and the square root of scan rate

**Fig.7** Effect of pH on anodic peak current ( I ) and anodic peak potential ( II ) for 20 μM PHZ at the *p*-ABSA/ZnO/GCE

**Fig.8** DPVs of different concentrations of PHZ (from a to i: 0.01 μM to 59.84 μM) at *p*-ABSA/ZnO/GCE in 0.10 M PBS (pH 8.0). The inset is the corresponding calibration curves of PHZ for peaks B



Remarkable enhancement effects on the oxidation peak currents of PHZ on the poly(*p*-ABSA)/ZnO modified electrode with the negative shift of the oxidation peak potentials.

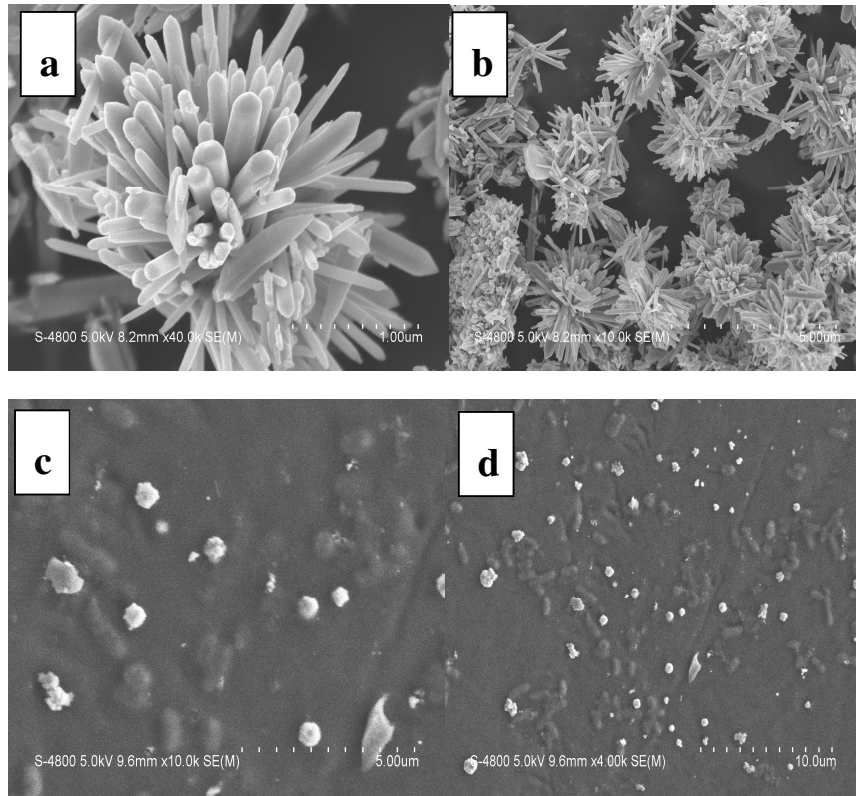


**Fig. 1**

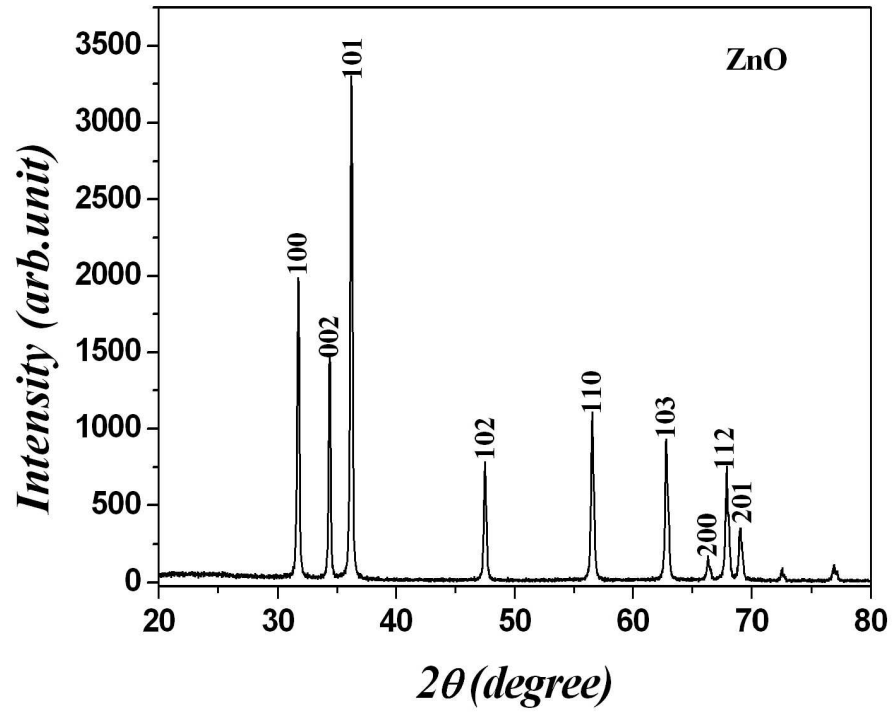


Fig. 2

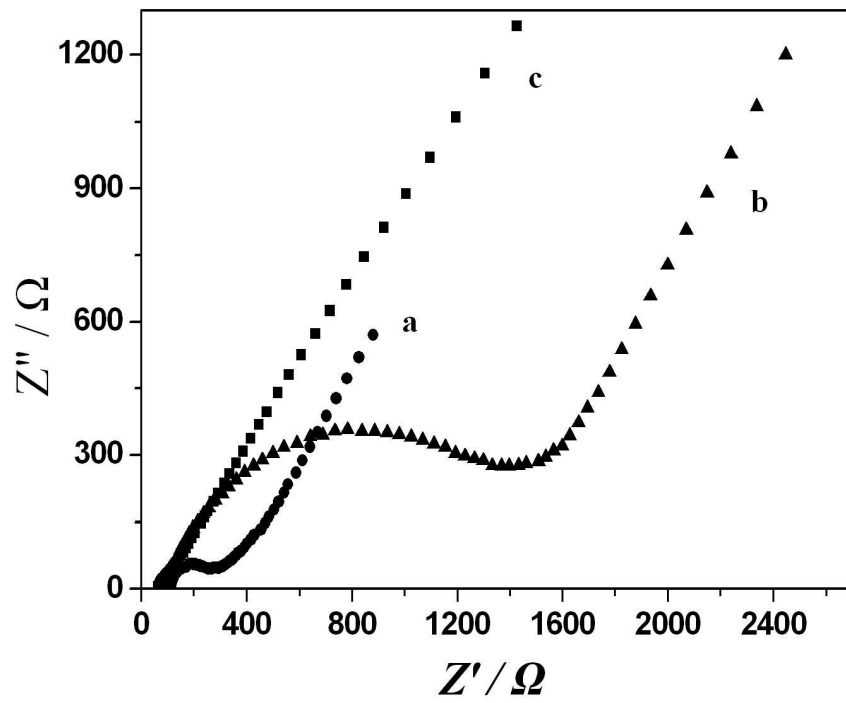


Fig. 3

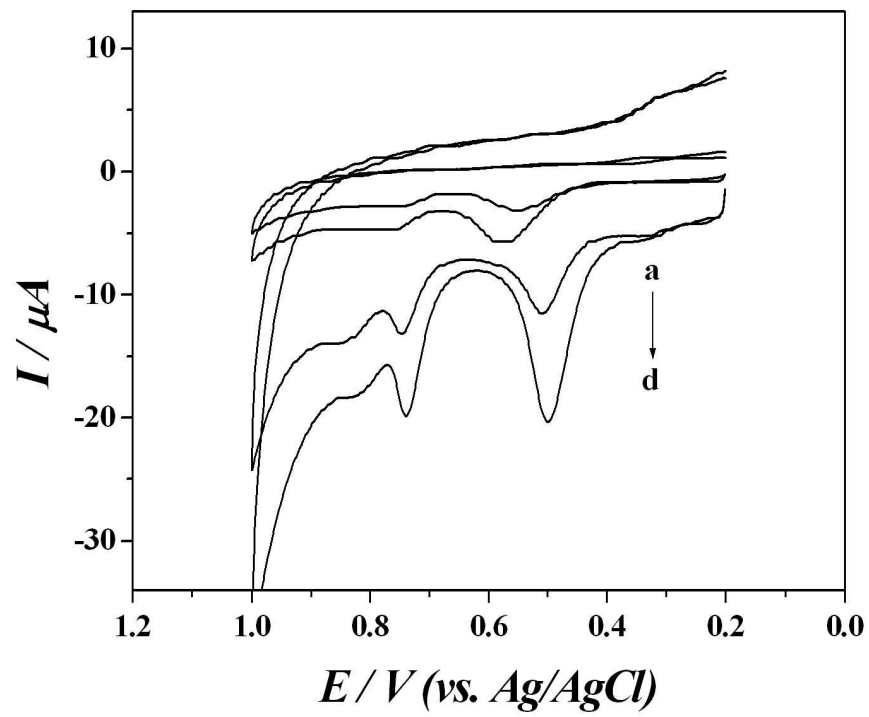


Fig. 4

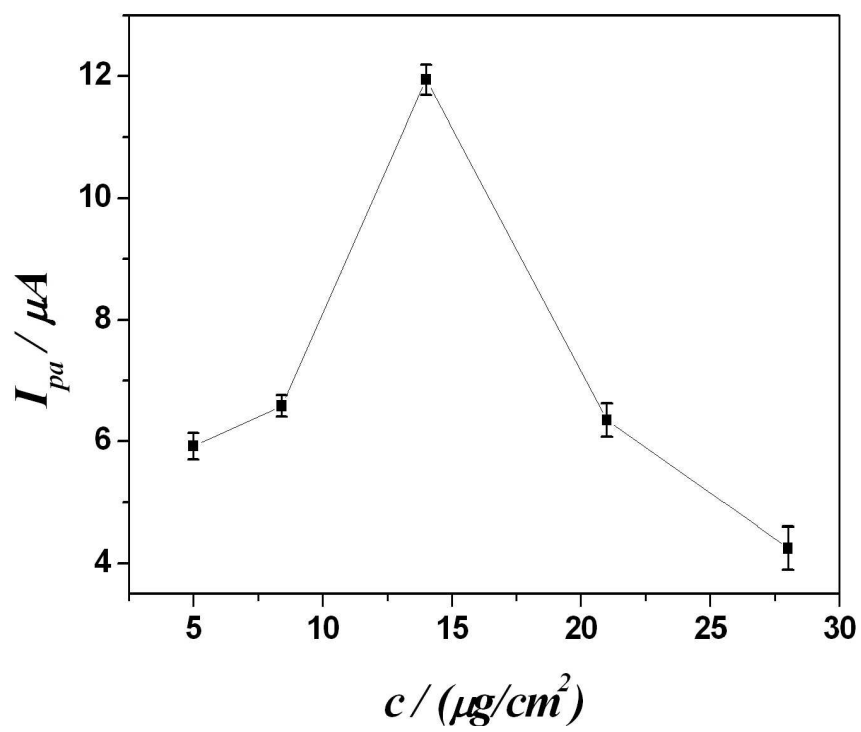


Fig. 5

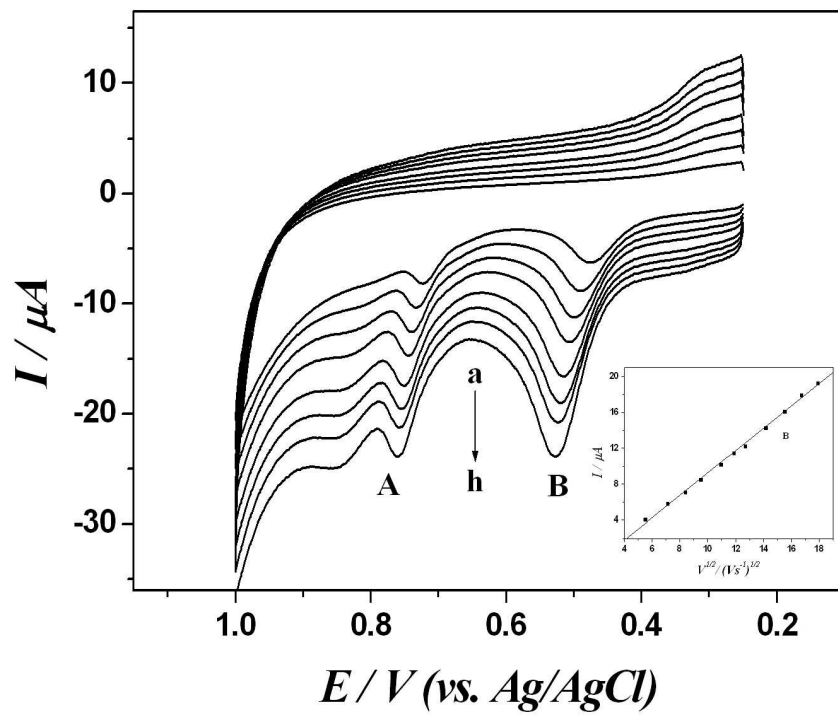


Fig. 6

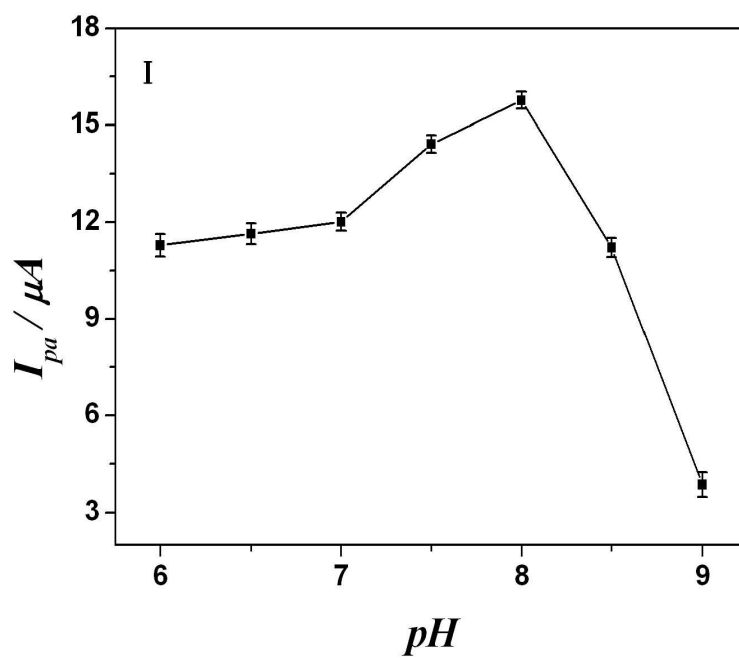


Fig. 7I

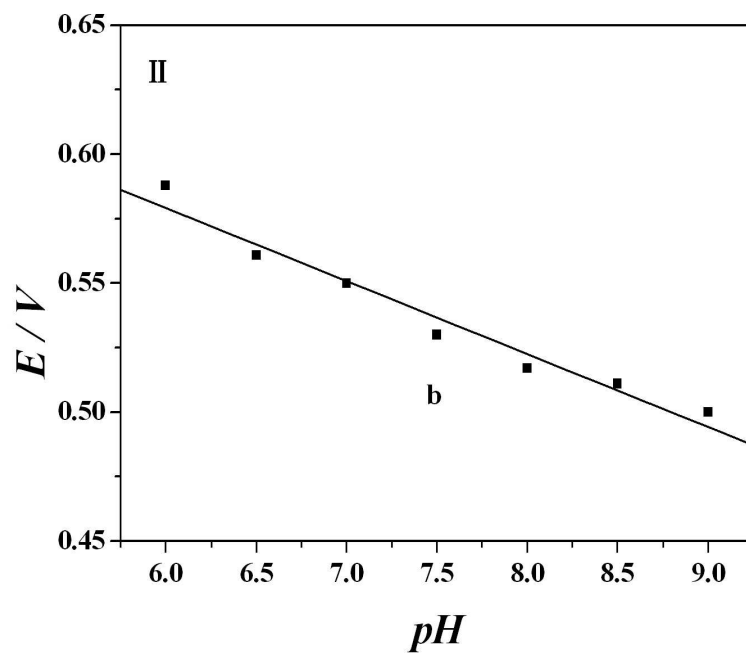


Fig. 7II

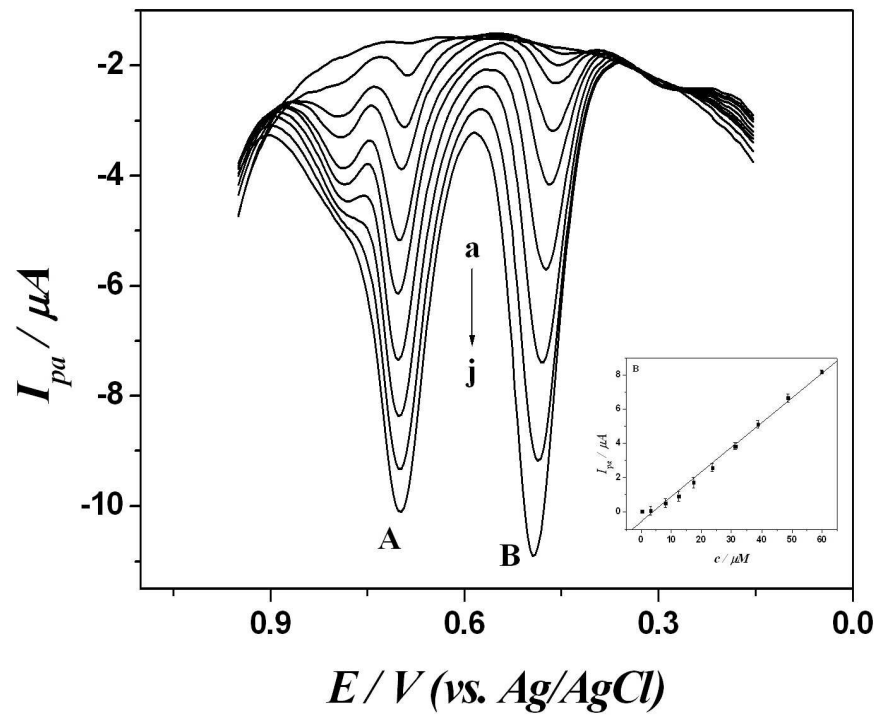


Fig. 8